Trans Indian Inst Met
https://doi.org/10.1007/s12666-020-01993-x

ORIGINAL ARTICLE

Rheological and Hindered Settling Studies on Bimodal Mixture Based on Multi-size and Multi-density Slurry: Multi-component Viscosity Model Development

Padhi Mandakini[1] · Bandi Sowmya[1] · Mohan Anand[1] · Mangadoddy Narasimha[1]

Received: 10 November 2019 / Accepted: 6 May 2020

Abstract The behavior of the fine solid mixture in a fluid depends critically on its rheological property. The rheological properties of a mixture change based on factors like particle size distribution, shape, density, etc. In this paper, two different minerals with distinct densities and similar size distribution with its mixture at different proportions (i.e., at 10–90% of magnetite/chromite ore: silica) were used for settling and rheological studies. Experiments were piloted using both mono-density and dual component mixture having poly-dispersed sample sets at different solids percentage (10–60%) for the hindered settling studies followed by rheological studies in the double-gap rheometer setup in a controlled shear rate method. The viscosity of the slurry decreased with an increased percentage of heavier particles in the mixture. Using the experimental data set, the effect of component density on the rheology of a particulate slurry mixture was assessed, and a multi-component viscosity mathematical model was developed.

Keywords Bimodal-poly-disperse · Density · Multi-component · Viscosity model · Settling behavior · Suspension rheology

✉ Mangadoddy Narasimha
narasimha@iith.ac.in

[1] Department of Chemical Engineering, Indian Institute of Technology Hyderabad, Sangareddy 502285, India

1 Introduction

The prediction of rheological properties of the solid–liquid slurry is essential for the control and operation of separation units in the mineral industry. Previous studies mainly focused on the mono-density slurry with different solids contents and had explored with varying parameters such as particle's size, shape, concentration, and surface characteristics [1–3]. The shear viscosity of bi-dispersed silica suspension was measured for three different sizes and different volume concentrations in the slurry; it was found that the viscosity decreases as a function of particle size [4]. Observations and improvements were attempted to understand the rheology of highly settling suspension like magnetite, ceramic beads, etc., [5, 6] in water. To address the settling problem, Ferrini et al. [7] supplied the material from the top to the annular region to maintain the suspension. Klein [5] used a double-gap cup and bob arrangement to avoid the sedimentation concern. He et al. [8] studied samples (at 5 different sizes) of magnetite slurry at low shear rates (1–300 s^{-1}) using HAAKE rotovisco RV20 rheometer and showed shear-thinning behavior for the slurry.

It is known that the blend of multi-size particles yields a suspension of higher fluidity or lower viscosity as compared to the mono-sized particles [2]. Farris et al. [9] developed a theory to explain the phenomenon of a well-dispersed multimodal slurry system. According to his theory, a bimodal slurry can be represented as the suspension of coarse particles in the media of homogeneous fine particles with the two fractions behaving independently. However, the model can not represent the inter-particle interaction with different size ratios. Probstein et al. [2] studied the coal slurry where coarse particles (200–300 microns) were added in a stable aqueous fine coal (2.3

Published online: 28 May 2020

microns). An application of the bimodal suspension model was explored and applied to coal-water suspension [10]. In the study, the coal colloidal particles of mean size 2.3 μm and 0.30 volume fraction were evaluated and compared with the coarse particles (200–300 μm) having 0.52 volume fraction, representing the confirmation of the bimodal model in the coal–water slurry. Similar bimodal coal slurry experiments were done with 2 low-rank coal in South Australia [11]. A wide spectrum of rheological behavior was observed, from Newtonian to Non-Newtonian, for low to high solids concentration of the fines (< 45 microns). Further, an optimum ratio of fines and coarse was found representing the Newtonian behavior, which has high solids loading.

Manjunath et al. [12] developed a model representing the yield stress of mixed flocculated suspension using alumina A16, alumina SR, and zirconia obtained from the rheology of concentrated suspensions. This model was represented in two parts where first part represented the structural model of yield stress including the effect of solids loading and size distribution, and the second part included the effect of solid's composition. Further, the effect of yield stress due to the inter-particle surface forces, particle size distribution, solid loadings, and compositions was analyzed and an aggregation index was proposed to represent the flow property [13]. However, due to the variation in the range of size distribution of different particles (approx. < 2 microns), the colloidal effect is found to be significant and the composition/density effect is difficult to be predicted by this method directly. Various studies on the dispersed suspension rheology have been attempted to understand the particle–particle forces based on short-range steric-forces and long-range hydrophobic colloidal forces [14]. These forces identify the van der Waals attractive and the electrostatic repulsive forces as particle–particle interactions, and the rheology of the dispersed suspension is explored under varying pH [15]. However, there is a lack of attention given to multimodal suspension systems having a significant effect of component density in a multi-component system. In the present work, a bimodal suspension system is considered consisting of similar particle size distribution and different density ratio of 1.39 ($\rho_{\text{Chromite ore}}/\rho_{\text{silica}}$) and 1.74 ($\rho_{\text{magnetite}}/\rho_{\text{silica}}$). The particles mixture is prepared at various proportions (as in 0%, 10%, 20%, 50%, 80%, 90%, and 100%) of magnetite/chromite ore in silica as supplementary fraction. The constant shear rate studies are performed at different solid fractions, and the mixture rheological behavior is compared with the pure components. The data obtained from the experiments are utilized to develop an empirical multi-component viscosity model.

2 Materials and Methods

2.1 Material Details and Sample Preparation

Three different types of samples having different densities 2.7, 3.7, and 4.5 g/cc for silica, chromite, and magnetite samples, respectively, were used for the tests. The size distribution (measured by Microtrac 3500) (Fig. 1a) and

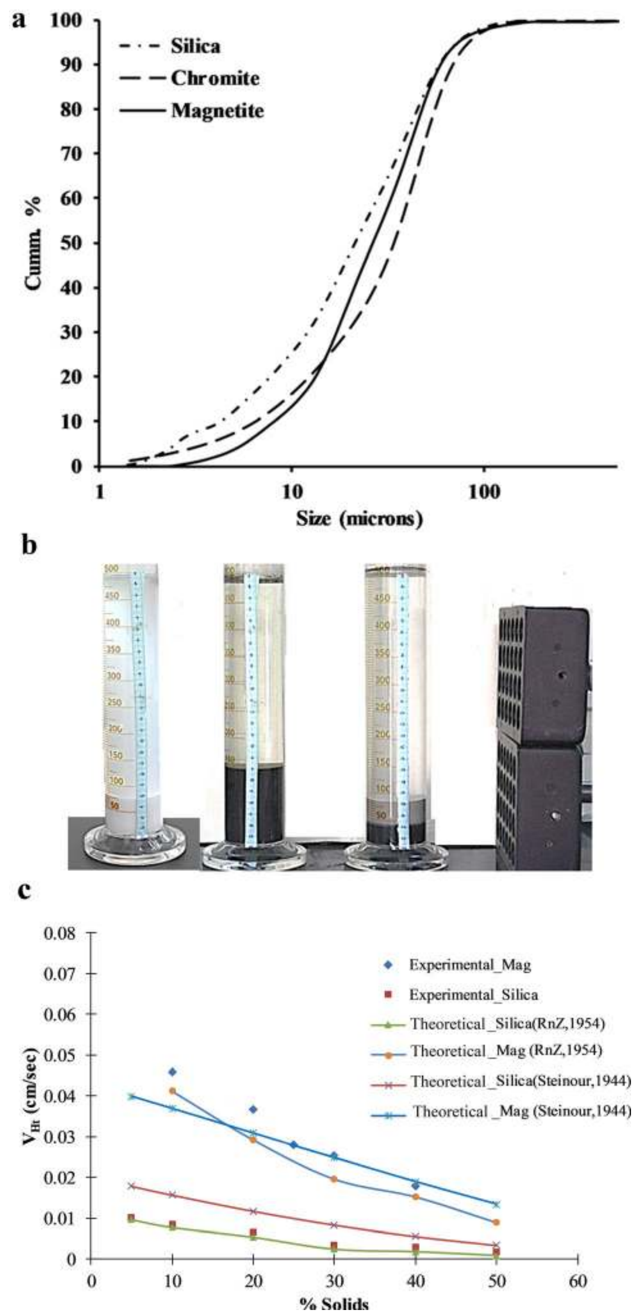

Fig. 1 **a** Size distribution of the particles—pure silica, pure magnetite, and chromite ore. **b** Experimental setup for the settling experiment **c** Comparison of experimental and theoretical hindered settling velocity of pure silica and magnetite

the shape determination were done to ensure the close shape similarity for the powders.

The mixture of bi-density (bimodal) and multi-sized (poly-dispersed) system was prepared by mixing the silica-magnetite and silica-chromite at various weight percentages (10; 20; 50; 80; 90% heavy particle) in water to reflect the multi-density effect in the system. The mixture homogeneity was ensured by stirring the feed sample in a magnetic stirrer prior to subjecting it to rheological study.

2.2 Experimental Setup and Methodology

2.2.1 Particle Settling Velocities

The primary objective of the study is to obtain the single component and multi-size settling data and to set proof of concept for understanding the hindering effect of the multi-density particles in a mixture slurry. In literature, the falling velocities (V_{Ht}) were defined for the velocities of a single spherical particle in an infinite medium (V_o).

A. The feed solids effect presented by Steinour [16] is given as:

$$\frac{v_{Ht}}{v_o} = \frac{(1-f_v)^2}{10^{1.82 * f_v}} \quad (1)$$

where f_v is the feed solids fraction, for specific cases having $f_v \geq 0.3$.

B. Rizhardson and Zaki [17] presented the uniform spherical particle fall velocity for particle settling in a tank with a diameter much larger than the particle diameter represented as:

$$V_{Ht} = V_o\left(\varepsilon^{4.65}\right) = V_o(1-C)^{4.65} \quad (2)$$

where ε is the voidage, C is the volume fraction of the solids in the suspension, and V_o is calculated from the stokes flow given as,

$$V_o = \frac{d^2(\rho_s - \rho)g}{18\mu} \quad (3)$$

To determine the settling rate in the laboratory, a transparent cylindrical column of known height details (scaled using graph sheet) was used to estimate the particle-water interface height with time (Fig. 1b). The silica and magnetite having different settling rates were observed under the naked eye and camera, respectively, to find the Δh versus Δt.

2.2.2 Bimodal Poly-dispersed Rheological Measurement

The setup from Anton Paar MCR301 rheometer with the double-gap geometry was utilized to access the suspension rheology. In the given geometry, the slurry was sandwiched between four walls, 2 inner and 2 outer, with the minimum gap as an external gap of 0.476 mm and an internal gap of 0.407 mm. To ensure the proper particle dispersion, the slurry was prepared and stirred by maintaining rpm followed by ultrasonic stirring for 30 s before injecting the sample into the system. The concept of pre-shear for the homogenization of the sample was carried at 1000 s^{-1} for 3 min to enable the highly settling particles in suspension before the viscosity measurement. The PSD adopted in this study for magnetite, chromite, and silica was in the range of 2–100 microns, consisting of 16 wt%, 14 wt%, and 21 wt% of fines below 10 microns, respectively. The majority of particles were in the micron range where the dominance of viscous and inertial forces is high. The parameters like viscosity, shear rate, shear stress, and torque were recorded at each shear rate using the software Rheoplus. The rheometer is equipped to auto-record the rotational speed of the rotor (rotating inner cylinder) (N, rpm) and the shear stress-related torque (M, mNm). The uncertainty analysis of the suspension rheogram was measured with 3 times repetition to obtain the suspension rheology (at the same program, i.e., the shear rate range, pre-shearing, and the number of data points/time exposed to get the flow curve). The mean standard deviation for pure silica, pure chromite, and its mixture at 80% and 50% chromite was found as $\leq 0.01\%$ (See Table 1). Since the observed mean standard deviation was very small to observe for the determined data, the error bars could not be presented in the rheograms shown in the manuscript.

3 Result and Discussion

3.1 Hindered Settling Studies of the Particles

The initial experiments are conducted for single density, pure components at varying solid concentrations (5–50 wt%). Figure 1c shows the comparison of theoretical variation of hindered settling velocities w.r.t. solids % using Richardson and Zaki [17] and Steinour [16] correlations. In all the cases, with increase in solids %, a decreased hindered settling velocity can be seen: this means that the hindrance effect is increasing with solids %. However, an isotope tracer-based detection approach will be more suitable to compare component settling rates in a mixture.

Table 1 Uncertainty analysis of rheograms for pure and mixture composition

Shear rate	SD			
	Only chromite	80% chromite	50% chromite	Only silica
250	0.00434	0.00282	0.00213	0.00130
232	0.00703	0.00455	0.00342	0.00207
206	0.00671	0.00435	0.00394	0.00194
180	0.00640	0.00415	0.00309	0.00179
155	0.00606	0.00392	0.00411	0.00163
129	0.00568	0.00365	0.00438	0.00146
103	0.00527	0.00336	0.00453	0.00128
77.8	0.00480	0.00302	0.00220	0.00107
52.2	0.01430	0.01892	0.01330	0.01430
26.6	0.01500	0.03000	0.02000	0.02340
1	0.03600	0.03155	0.04345	0.05400
MSD	0.010144	0.010025	0.009505	0.009477

3.2 Poly-dispersed: Mono-density Rheology

The analysis of the pure silica and pure magnetite illustrates the change in behavior based on the solids content. For specified shear rates, the shear stresses of the pure magnetite are observed to attain a higher magnitude compared to the silica (Fig. 2). The magnitude of apparent viscosity is higher for the lighter particle having the same solid fractions as compared to the heavier particle slurry. The rheograms show the shear-thinning behavior depicting a non-Newtonian fluid.

The yield stress recorded has been found to have a higher magnitude for magnetite compared to silica. The slope of the rheogram for either of the slurry sample increases by adding more solids to the system. However, magnetite has highly settling behavior: at higher solids and low shear rates, the hydrodynamics of the slurry changes significantly and this can be noticed in Fig. 2a.

3.3 Poly-dispersed: Bimodal Rheology

3.3.1 Artificial Mixture

With the artificial mixture, which represents a bimodal system, it is observed that with an increase in the proportion of magnetite, the shear stress curve attains a higher slope compared to the pure lighter particle slurry. With the increased colloidal forces at higher solid % and fines fractions in the particle size distribution, an increased viscosity is predicted. At a very low volume fraction, the rheogram attains nearly Newtonian behavior, whereas with the increase in the solids, the shear-thinning behavior is observed, similar to the previous pure component studies (Fig. 2c).

This phenomenon is attributed to the inherent interaction of the particles in the mixture, altering the packing of the particle to be compact due to the change in the internal arrangements. At higher shear rates, the viscous forces affect the slurry structure by distorting the arrangements

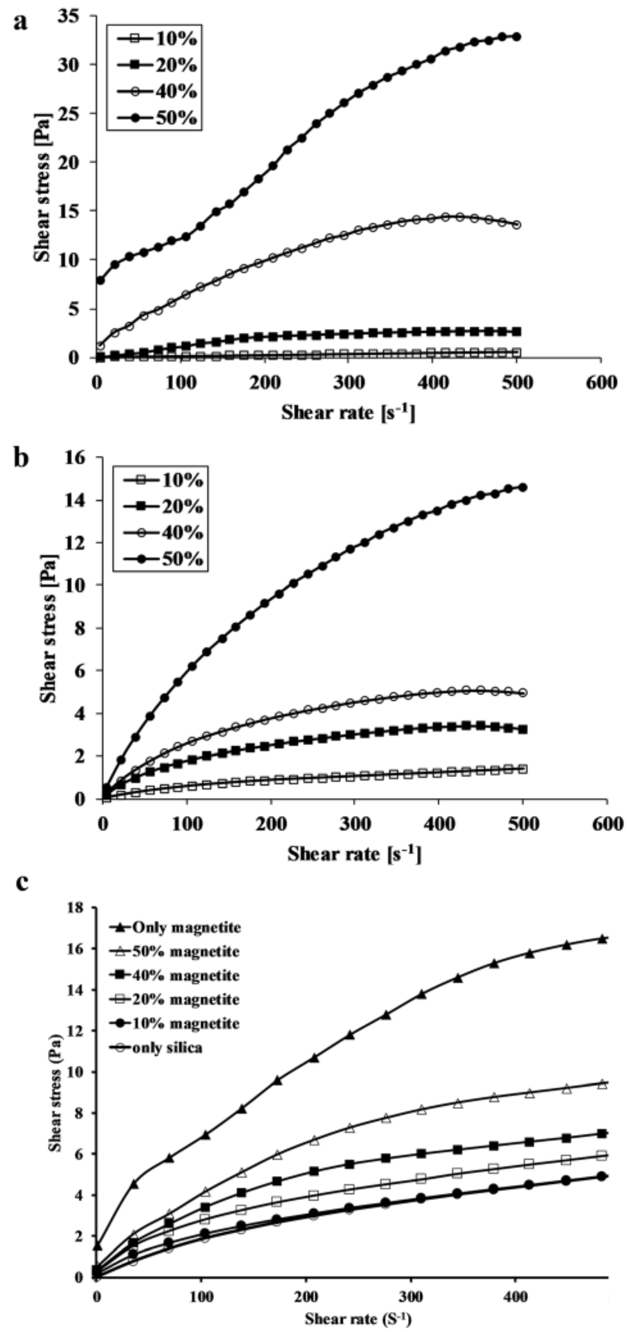

Fig. 2 Illustration of rheograms of poly-dispersed—mono-density particles **a** pure Magnetite and **b** pure silica **c**, **a** CSR rheograms of magnetite and silica at various proportions of magnetite and 50 wt% total solids

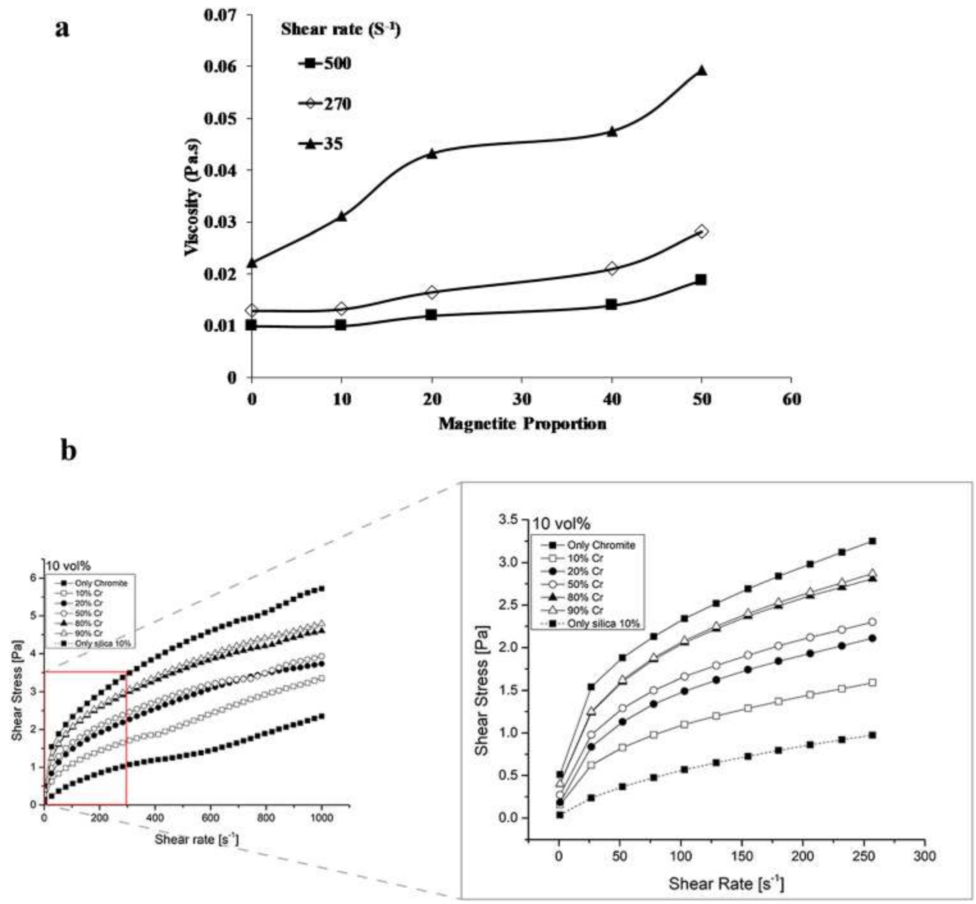

Fig. 3 **a** Comparison of apparent viscosity at various shear rates with changing magnetite proportions in the slurry. **b** CSR rheograms of chromite ore and silica at the various proportion of chromite and 10% total solids

and hence leading to the pseudo-plastic fluid behavior. The comparison of apparent viscosity at various shear rates shows that with the increase in shear rates, the viscosity decreases (Fig. 3a), which can be as a result of the interaction of the highly settling particles at lower shear rates; whereas, at higher shear rates, it forms layers of particles, which slide over each other easily. Similar experiments have been conducted using natural ore (chromite) as a component and presented in Fig. 3b.

As the samples considered have similar size distribution, the differences observed are the result of varying densities. In addition, irrespective of the solid's content, the fines in the slurry have a high specific surface area, which reduces the inter-particle distance and increases the viscosity at lower shear rates.

3.4 Exploration of a Model for Mixture Slurry

The analyzed viscosity data from the above experiment are utilized to quantify the relative viscosity of poly-dispersed size and bi-density particles system based on the study by Farris [9], which demonstrates that the relative viscosity of bimodal suspension can be related to individual component contributions as given below

$$\eta_{r\text{mix}} = \frac{\eta_{\text{mix}}}{\eta_o} = \left(\frac{\eta_f}{\eta_o}\right)\left(\frac{\eta_c}{\eta_f}\right) = \eta_{\text{fr}}\eta_{\text{cr}} \tag{4}$$

where η_{fr} is the relative viscosity of fines defined as the relative viscosity of the fine suspension with respect to the viscosity of suspending fluid. In addition, the η_{cr} represents the coarse contribution of the viscosity relative to fine particle suspension.

Further, the slurry viscosity depends on the volume fraction of solids as referred by many parts of research in the past, starting from Einstein [18]. Narasimha et al. [19] have modified the similar model given by Ishii-Mishima [20] with the fine fractions (i.e., < 38 microns) particle size distribution while modeling the slurry viscosity in hydrocyclones as shown below.

$$\frac{\eta_m}{\eta_w} = F_{-38\mu}^{0.39} * \left(1 - \frac{\alpha_p}{0.62}\right)^{-1.55} \tag{5}$$

Hence, in the proposed model, the volume fraction and fines effects on the viscosity is accounted for determining the mixture viscosity based on Eq. 5. Initially, the lighter component viscosity is obtained at a given volume fraction, followed by predicting the heavy particle slurry viscosity relative to the lighter particle slurry. Finally, the multi-component viscosity model can be represented as,

$$\eta_r = \frac{\eta_H}{\eta_w} = (\eta_{\mathrm{lw}})\left(\frac{\eta_H}{\eta_{\mathrm{lw}}}\right) = \left(\frac{\eta_l}{\eta_w}\right)\left(\frac{\eta_H}{\eta_{\mathrm{lw}}}\right) = \eta_{\mathrm{Lr}}\eta_{\mathrm{Hr}} \quad (6)$$

where $\eta_{r\mathrm{mix}}$, η_{lr} or η_{lw} and η_{Hr} or $\eta_{H-\mathrm{lw}}$ represents the relative viscosity for mixture, lighter component slurry viscosity, and heavier component viscosity in a lighter component slurry. Further, it can be expanded as

$$\frac{\eta_L}{\eta_w} = k_1 * \left(1 - \frac{\alpha_{tL/(L+w)}}{0.62}\right)^{-1.55} \quad (7)$$

$$\frac{\eta_H}{\eta_{\mathrm{lw}}} = k_2 * \left(1 - \frac{\alpha_{tH/(H+L+w)}}{0.62}\right)^{-1.55}. \quad (8)$$

In Eq. (8), $k_2 = k' * k_2'$. The k_1, k_2' are constants representing the $F^{0.39}_{-38\mu}$ (fines below 38 microns, considered as 0.46, 0.32, and 0.41 for the adapted PSD of silica, chromite ore, and magnetite, respectively). In addition, the constant k' is introduced as an interaction parameter obtained by considering the total intrinsic viscosity [21, 22] by the lighter and heavier particle slurry which represents the lighter and heavier particle solute concentration effect on the mixture slurry viscosity in total, defined as,

$$[\eta] = \frac{\eta - \eta_f}{\eta_{f*}\phi_L} + \frac{\eta - \eta_f}{\eta_{f*}\phi_{H-\mathrm{lw}}} \text{ and } k' = [\eta]^{1.5}. \quad (9)$$

In Eq. (9), $[\eta]$, η_{f}, and η are intrinsic viscosity, fluid medium viscosity, and slurry viscosity of the slurry with $\Phi_{\mathrm{H\text{-}lw}}$ heavier particle and Φ_{L} lighter particle solids content in the mixture slurry. The calculation of the η is done by the definition of the Ishii-Mishima viscosity model (see Eq. 5, without F_{-38} fraction). The power '1.5' is fitted by regression analysis, as an exponential constant. In Fig. 4a and b, the Pareto plots present the regression fitting for the model data and the validation data, respectively.

The presented data are a representation of 54 data set from various combinations of magnetite-silica and chromite-silica particles. Out of the 54 data set, 33 have been utilized to formulate the regression-based semi-empirical model and 21 data set have been used for the validation in the current study. The estimated R^2 for the model-building data and validation data is found to be 0.91823 and 0.8422, respectively. Table 2 represents the regression statistics of the prediction and validation data set. The precision of the regression coefficient can be assessed by the standard error estimated, i.e., found as 0.0033 and 0.008 for the model-building data and validated data, respectively. Further, the

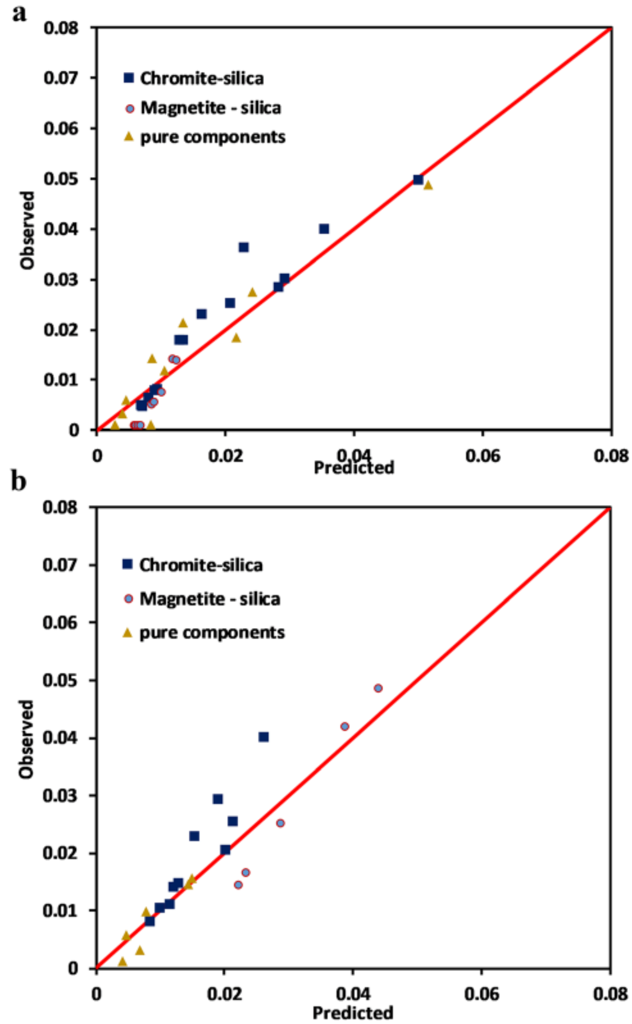

Fig. 4 **a** Comparison of the experimental and predicted data set for the relative viscosity of the mixture data set used for the model building **b** validation of the predicted data with new experimental data set

Table 2 Regression statistics

Regression statistics		
Predicted data		Validated data
R square	0.91823	0.84222
Standard error	0.00447	0.00517
Observations	33	21

significance of F value in the ANOVA analysis is found to be < 0.05 (see Table 3), i.e., the values used for the model prediction are a better fit. Hence, this model can be used to predict a similar set of multi-component viscosity data.

However, to make the model more generic and robust, additional analysis of the flow curves for a wide range of density difference systems is planned and is in progress.

Table 3 (a) ANOVA for the prediction data set, (b) ANOVA for the validation data set

	df	SS	MS	*F*	Significance *F*
(a)					
Regression	1	0.008179	0.008179	713.2197	5.836E−23
Residual	31	0.000355	1.15E−05		
Total	32	0.008534			
	df	SS	MS	*F*	Significance *F*
(b)					
Regression	1	0.002713	0.002713	101.4214	4.69E−09
Residual	19	0.000508	2.68E−05		
Total	20	0.00322			

4 Conclusions

The settling experiment shows that the denser particle tends to approach the dead bed faster as compared to the lighter particle in a mixture, thus increasing the interaction in the slurry system. The rheological study of pure, multi-sized, and bi-density particle slurry displays the change in rheological property with the change in the composition of the mixture. The interaction of the heavier particle in the lighter particle slurry system at lower shear rates is observed to be substantial and changes with the change in the proportions of mixture. The relative model proposed for mixture viscosity implies the higher impact of the heavy particles in the lighter particle slurry, which can also affect the multi-component particles separation when encountered in various industrial processes. Further, the obtained model can be utilized for developing computational/mathematical models for the multi-component system.

Acknowledgements The authors would like to thank Indian Institute of Technology Hyderabad for providing the facilities and DST-SERB (EMR/2016/00378/046) Grant for financial support.

References

1. Luckham P F, and Ukeje M A, *J. Colloid Interface Sci.* **220**, (1999) 347.
2. Probstein R F, *J. Rheol.* **38** (1994) 811.
3. Yuan J, and Murray H H, *Appl. Clay Sci.* **12** (1997) 209.
4. Zaman A A, and Moudgil B M, *J. Rheol.* **42** (1998) 21.
5. Klein B, Partridge S J, and Laskowski J S, *Coal Prep.* **8** (1990) 123.
6. Gustafsson J, Toivakka M, and Koskinen K K, *Annu. Trans. Nord. Rheol. Soc* **13** (2005) 277.
7. Ferrini F, Ercolani D, De Cindio B, Nicodemo L, Nicolais L, and Ranaudo S, *Rheol. Acta* **18** (1979) 289.
8. He Y B, and Laskowski J S, *Miner. Eng.* **7** (1994) 209.
9. Farris R J, *Trans. Soc. Rheol.* **12** (1968) 281.
10. Sengun M Z, and Probstein R F, *Rheol. Acta* **28** (1989) 382.
11. Nguyen Q D, Logos C, Semmler T, *Coal Prep.* **18** (1997) 185.
12. Subbanna M, Pradip, and Malghan S G, *Chem. Eng. Sci.* **53** (1998) 3073.
13. Subbanna M, Kokil S, Kapur P C, Pradip, and Malghan S G, *Langmuir* **14** (1998) 7364.
14. Leong Y -K, Boger D V, Scales P J, Healy T W, and Buscallb R, *J. Chem. Soc. Chem. Commun.* **7** (1993) 639.
15. Johnson S B, Franks G V, Scales P J, Boger D V, and Healy T W, *Int. J. Miner. Process.* **58** (2000) 267.
16. Steinour H H, *Ind. Eng. Chem.* **36** (1944) 840.
17. Richardson J F, and Zaki W N, *Chem. Eng. Sci.* **3** (1954) 65.
18. Einstein A, *Ann. Phys.* **34** (1911) 591.
19. Narasimha M, Mainza A N, Holtham P N, Powell M S, and Brennan M S, *Int. J. Miner. Process.* **133** (2014) 1.
20. Ishii M, and Mishima K, *Nucl. Eng. Des.* **82** (1984) 107.
21. Rubio-Hernández F J, Ayúcar-Rubio M F, Velázquez-Navarro J F, and Galindo-Rosales F J, *J. Colloid Interface Sci.* **298** (2006) 967.
22. Smith T L, and Bruce C A, *J. Colloid Interface Sci.* **72** (1979) 13.